Pure Appl. Chem., Vol. 81, No. 9, pp. 1555–1568, 2009.
doi:10.1351/PAC-CON-08-09-05

Thermodynamics of trivalent actinides and neodymium in NaCl, $MgCl_2$, and $CaCl_2$ solutions: Solubility, hydrolysis, and ternary Ca–M(III)–OH complexes*

Volker Neck[1,‡], Marcus Altmaier[1], Thomas Rabung[1], Johannes Lützenkirchen[1], and Thomas Fanghänel[2]

[1]Forschungszentrum Karlsruhe, Institut für Nukleare Entsorgung, P.O. Box 3640, D-76021 Karlsruhe, Germany; [2]European Commission, JRC, Institute for Transuranium Elements, P.O. Box 2340, D-76125 Karlsruhe, Germany

Abstract: Known data on the solubility of $Am(OH)_3(s)$ and the hydrolysis of Am(III) and Cm(III), additional information from an extensive solubility study with $Nd(OH)_3(s)$ in NaCl, $MgCl_2$, and $CaCl_2$ media of various ionic strengths and spectroscopic (time-resolved laser fluorescence spectroscopy, TRLFS) data for Cm(III) in alkaline $CaCl_2$ solutions are used to evaluate a comprehensive set of standard-state equilibrium constants and ion interaction parameters for the specific ion interaction theory (SIT) and Pitzer equations at 25 °C. The thermodynamic model takes into account the analogous solubility and hydrolysis behavior of trivalent actinides and Nd(III) and covers the entire pH range in dilute to concentrated NaCl, $MgCl_2$, and $CaCl_2$ solutions. In alkali chloride/hydroxide solutions, the formation of the tetrahydroxide complex $M(OH)_4^-$ requires OH^- concentration above 3 mol l^{-1}, whereas in alkaline $CaCl_2$ solutions (at $pH_c < 12$) M(III) complexes with four and six hydroxide ligands are formed. Similar as the recently detected ternary Ca–M(IV)–OH complexes $Ca_3[Zr(OH)_6]^{4+}$ and $Ca_4[Th(OH)_8]^{4+}$, these complexes are stabilized by the association of Ca^{2+} ions. The solubility and hydrolysis of Am(III), Cm(III), and Nd(III) in both Ca-free and -containing solutions is consistently described with a model including the ternary Ca–M(III)–OH complexes $Ca[M(OH)_3]^{2+}$, $Ca_2[M(OH)_4]^{3+}$, and $Ca_3[M(OH)_6]^{3+}$.

Keywords: americium; curium; hydrolysis; neodymium; Pitzer model; plutonium; SIT; solubility; ternary complexes.

INTRODUCTION

The solubility and aqueous speciation of actinides in chloride solutions is of particular interest with regard to the safety of nuclear waste storage in underground salt mines like the Waste Isolation Pilot Plant (WIPP) in the United States or the Asse salt mine in Germany. Intrusion of water is supposed to yield NaCl- or $MgCl_2$-dominated salt brines. In order to minimize actinide solubilities, brucite-based backfill material has been proposed to buffer pH by magnesium hydroxide $Mg(OH)_2(s)$ or hydroxychloride $Mg_2(OH)_3Cl{\cdot}4H_2O(s)$ at values of pH ≈ 9 [1,2] and to scavenge carbonate due to the limited solubility

*Paper based on a presentation at the 13th International Symposium on Solubility Phenomena and Related Equilibrium Processes (ISSP-13), 27–31 July 2008, Dublin, Ireland. Other presentations are published in this issue, pp. 1537–1614.

‡Corresponding author: E-mail: neck@ine.fzk.de

of magnesium carbonates. In $MgCl_2$ brines, the corrosion of cementitious waste forms can lead to $CaCl_2$-dominated solutions buffered at pH ≈ 12 by calcium hydroxide $Ca(OH)_2$(s) or hydroxychlorides, $Ca_4(OH)_6Cl_2 \cdot 13H_2O$(s) and $Ca_2(OH)_2Cl_2 \cdot H_2O$(s) [2]. Under redox conditions controlled by corroding steel containers of nuclear waste packages, the most important actinides will be in the oxidation states An(III) (Am, Cm, Pu) or An(IV) (Th, U, Np, Pu) [3–7]; for plutonium, solid PuO_2(s, hyd) is expected in equilibrium with aqueous Pu(IV) and Pu(III) species [8].

Thermodynamic data for the solubility and hydrolysis of tri- and tetravalent actinides in chloride solutions belong to the key values for performance assessment calculations. However, the data selected in the critical reviews of the Organization for Economic Cooperation and Development (OECD)/Nuclear Energy Agency (NEA-TDB) [3–7] are usually based on experimental studies in $NaClO_4$ or NaCl media. There is a lack of systematic studies in dilute to concentrated $MgCl_2$ and $CaCl_2$ solutions. Moreover, our recent solubility measurements and spectroscopic studies with Zr(IV), Th(IV), Pu(IV), Nd(III), and Cm(III) in alkaline $CaCl_2$ solutions [9–12] revealed a hitherto unknown phenomenon, the formation of ternary Ca–M–OH complexes with unusually high numbers of OH^- ligands. The solubilities of $ZrO_2 \cdot xH_2O$(s) at pH = 10–12 in 0.1–2.0 M $CaCl_2$ and of $ThO_2 \cdot xH_2O$(s) at pH = 11–12 in 0.5–4.5 M $CaCl_2$ are raised to unexpectedly high values by the formation of the complexes $Ca_3[Zr(OH)_6]^{4+}$ and $Ca_4[Th(OH)_8]^{4+}$, respectively, which could be identified and characterized by extended X-ray absorption fine structure spectroscopy (EXAFS) [9,10]. The equilibrium constants for these complexes were calculated in [10] with the specific ion interaction theory (SIT) [13] recommended in the NEA-TDB for ionic strength corrections. However, highly saline $MgCl_2$ or $CaCl_2$ solutions with ionic strengths up to 16 mol kg^{-1} are far beyond the validity range of the SIT ($I < 4$ mol kg^{-1}). The ion interaction model of Pitzer [14] is applicable to high ionic strength and used in geochemical modeling codes like EQ3/6 or Geochemist's Workbench (GWB). Therefore, it was recently used to model the data for the An(IV) complex $Ca_4[An(OH)_8]^{4+}$ (An = Th and Pu) at high $CaCl_2$ concentrations [12]. Standard-state equilibrium constants and ion interaction parameters for the An(III) species formed in neutral and alkaline NaCl, $MgCl_2$, and $CaCl_2$ solutions will be presented in this paper.

SOLUBILITY AND HYDROLYSIS OF TRIVALENT ACTINIDES—STATE OF THE ART

Trivalent actinides and lanthanides show pronounced analogies in most chemical properties, systematic trends in the thermodynamic data and equilibrium constants often correlate with the ionic radius [6,15,16]. Considering the similar ionic radii of Nd^{3+}, Pu^{3+}, Am^{3+}, and Cm^{3+} (111, 112, 110, and 109 pm, respectively, at coordination number CN = 8 [16,17]), it is not surprising that the real differences between the formation constants of their aqueous complexes are smaller than the experimental uncertainties [6,18]. Due to specific experimental difficulties or the lack of appropriate experimental methods for Am(III) or Pu(III) at trace concentration levels, it is more convenient to use oxidation-state analogs, for instance, Cm(III) with fluorescence properties that allow investigations by time-resolved laser fluorescence spectroscopy (TRLFS) at concentrations below 10^{-7} mol l^{-1} [19]. For reasons of easier handling, the non-radioactive lanthanides Nd(III) and Eu(III) are also often studied as analogs for the trivalent actinides.

The literature on the solubility and hydrolysis of Am(III), Cm(III), and Pu(III) is critically discussed in NEA-TDB reviews [4–6]. In the absence of carbonate, silicate, or phosphate, the solubility-limiting solid phase is the An(III) hydroxide:

$$An(OH)_3(s) + 3H^+ \Leftrightarrow An^{3+} + 3H_2O$$

$$\text{with } {}^*K^\circ_{s.0} = [An^{3+}]\ \gamma_{An^{3+}}\ ([H^+]\ \gamma_{H^+})^{-3}\ (a_w)^3 \quad (1)$$

At pH 5–13 in $NaClO_4$ and NaCl solutions, Am(III), Cm(III), and Pu(III) form only mononuclear hydrolysis species $An(OH)_n^{3-n}$ with n = 1–3, there is no indication for oligomers $An_m(OH)_n^{3m-n}$ [4–6]:

$$An^{3+} + nH_2O \Leftrightarrow An(OH)_n^{3-n} + nH^+$$

$$\text{with } {}^*\beta^\circ_{1n} = [An(OH)_n^{3-n}]\ \gamma_{An(OH)n^{3-n}}\ ([H^+]\ \gamma_{H^+})^n\ ([An^{3+}]\ \gamma_{An^{3+}})^{-1}(a_w)^{-n} \quad (2)$$

where ${}^*K^\circ_{s,0}$ and ${}^*\beta^\circ_{1n}$ are the equilibrium constants at zero ionic strength ($I = 0$), $[i]$ is the concentration and γ_i the activity coefficient of species i, and a_w is the activity of water. Activity coefficients may be calculated with the SIT as in the NEA-TDB reviews or with the Pitzer model. Since small differences in the ionic radii of aquo ions or complexes of equal charge and symmetry have only a slight effect on the activity coefficients, ion interaction coefficients (both SIT and Pitzer parameters) for Nd^{3+} and An^{3+} ions (An = Pu, Am, Cm) and their analogous aqueous complexes can be set equal [6,20–22].

Solubility of $Am(OH)_3$(s) and aqueous speciation at high pH

There are numerous solubility studies with Am(III) hydroxides at pH 6–13 in carbonate-free $NaClO_4$ and NaCl solutions [23–28]. Figure 1a shows experimental data determined after 1.5–2 nm ultrafiltration at I = 0.1 M [23–26] or in dilute solutions [27]. The thermodynamic properties of the solid hydroxide and hence the solubility depends on the degree of crystallinity, i.e., on the particle/crystallite size which is affected by aging or ripening processes and by self-irradiation effects from the α-activity of americium. The solubility calculated with the data selected in the NEA-TDB [6] for crystalline or aged $Am(OH)_3$(s) ($\lg {}^*K^\circ_{s,0}$ = 15.6 ± 0.6), amorphous $Am(OH)_3$(am) precipitates ($\lg {}^*K^\circ_{s,0}$ = 16.9 ± 0.8) and the complexes $Am(OH)_n^{3-n}$ ($\lg {}^*\beta^\circ_{1n}$ = –7.2 ± 0.5, –15.1 ± 0.7 and –26.2 ± 0.5 for n = 1, 2, and 3, respectively) is represented by the lines in Fig. 1a. The use of the notation "crystalline" and "amorphous" to describe a solid phase and thereby its solubility is an oversimplification. The X-ray diffraction (XRD) data give only information of the bulk structure, while the solubility is determined by the surface characteristics or by fractions of smaller ("amorphous") particles included in a bulk crystalline solid [6,7].

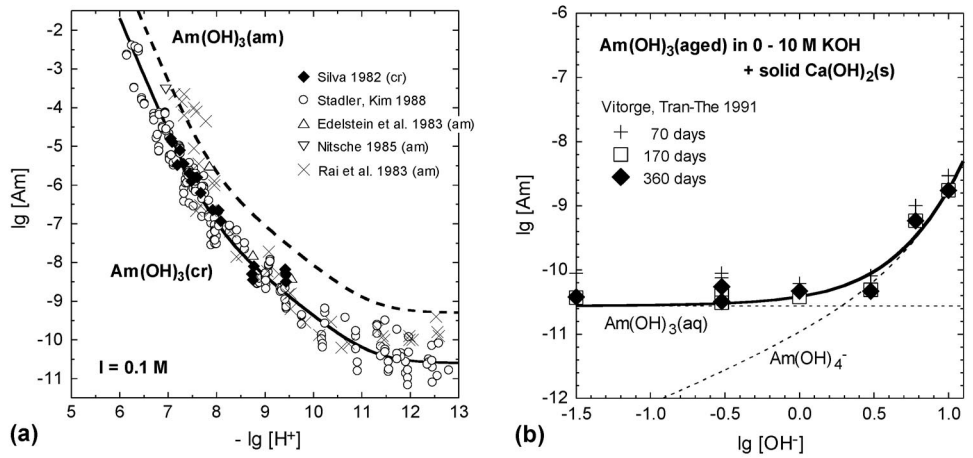

Fig. 1 Solubility of Am(III) hydroxide at 25 °C. (a) Crystalline/aged $Am(OH)_3$(s) (solid line) and amorphous $Am(OH)_3$(s) (dashed line) at I = 0.1 M (exp. data from [23–27]); (b) Aged $Am(OH)_3$(s) in 0–10 M KOH with additions of solid $Ca(OH)_2$(s) [29]. The SIT calculations are based on data selected in the NEA-TDB [6] and in this work for $Am(OH)_4^-$ (see text).

The low americium concentrations at pH > 10, usually ascribed to the equilibrium between $Am(OH)_3$(s) and the neutral aqueous complex $Am(OH)_3$(aq), are rather scattered but at a constant level (lg [Am] = –9.3 ± 1.0 for $Am(OH)_3$(am) and –10.6 ± 0.8 for aged or crystalline $Am(OH)_3$(s) [6]).

Solubility studies in NaCl–NaOH, $NaClO_4$–NaOH, pure NaOH, or KOH solutions up to pH 14 show no indication for the formation of an anionic hydroxide complex $Am(OH)_4^-$ that would increase the solubility at high pH [4,6]. In extremely alkaline solutions ($[OH^-] > 3$ M), an increase of the americium concentration has been observed by Vitorge and Tran-The [29] who measured the solubility of fresh and aged Am(III) hydroxide precipitates in 0–10 M KOH with additions of solid $Ca(OH)_2$(s) to scavenge carbonate (Fig. 1b). Because of the high and variable ionic strength, these results were not evaluated and selected in the NEA-TDB reviews [4,6]. As shown in Fig. 1b, the solubility increase in 3–10 M KOH can be described with an equilibrium constant of $\lg K^\circ_{3-4} = -0.5 \pm 0.4$ for the reaction $Am(OH)_3(aq) + OH^- \Leftrightarrow Am(OH)_4^-$ (corresponding to $\lg {}^*\beta^\circ_{14} = -40.7 \pm 0.7$) and ion interaction (SIT) coefficients of $\varepsilon[Am(OH)_3(aq), K^+/OH^-] = 0$, $\varepsilon(OH^-, K^+) = 0.09 \pm 0.01$ kg mol^{-1} [3–6] and $\varepsilon[Am(OH)_4^-, K^+] = -0.03 \pm 0.05$ kg mol^{-1}.

Aqueous speciation by TRLFS with Cm(III)

The sensitive TRLFS is often used to determine the aqueous speciation and complex formation constants of Cm(III) at trace concentration levels (c.f., Fanghänel and Kim [19]). In acidic chloride solutions up to 5 M NaCl and 2 M $CaCl_2$, the TRLFS emission band of the Cm^{3+}(aq) ion with the maximum at $\lambda_{max} = 593.8$ nm is not affected [30,31]. The formation of chloride complexes requires higher Cl^- concentrations; in 4 M $CaCl_2$ about 50 % of the curium is present as $CmCl^{2+}$ ($\lambda_{max} = 594.9$ nm) and $CmCl_2^+$ ($\lambda_{max} = 598.3$ nm) [30]. In TRLFS studies on the hydrolysis of Cm(III) in neutral and alkaline 0.1 M $NaClO_4$ [32] and dilute to concentrated NaCl [31], only the emission spectra of $Cm(OH)^{2+}$ ($\lambda_{max} = 598.8$ nm) and $Cm(OH)_2^+$ ($\lambda_{max} = 603.5$ nm) were observed. Because of the low solubility at pH > 10, neither the complex $Cm(OH)_3$(aq), which is expected to dominate the speciation at pH = 11–14, nor the complex $Cm(OH)_4^-$ could be detected. A TRLFS study of 10^{-8} M Cm(III) in 0.01–4.0 M NaOH showed no discernible fluorescence emission spectra and in 5.0–7.5 M NaOH only a weak, broad fluorescence band appeared between 600 and 625 nm [33]. The same observation was made in 5 M NaCl–NaOH with $[OH^-] = 1$–4 M [11]. Almost all of the curium is present as $Cm_m(OH)_{3m}$ polymers or colloidal $Cm(OH)_3$(am), which shows no fluorescence (complete quenching) [33,34].

In alkaline $CaCl_2$ solutions, the chemical and spectroscopic behavior of Cm(III) is strikingly different. Rabung et al. [11] recorded TRLFS spectra in 0.1–3.5 M $CaCl_2$ at pH 11–12 and observed hitherto unknown Cm(III) emission bands caused by complexes with three, four, and six OH^- ligands. The emission bands of these complexes are regularly shifted to higher wavelength ($\lambda_{max} = 607.5$, 609.9, and 614.7 nm, respectively) compared to those of Cm^{3+}(aq) ($\lambda_{max} = 593.8$ nm), $Cm(OH)^{2+}$ ($\lambda_{max} = 598.8$ nm) and $Cm(OH)_2^+$ ($\lambda_{max} = 603.5$ nm). These complexes, absent in NaCl–NaOH solutions, are stabilized by the association of Ca^{2+} ions, i.e., by the formation of ternary complexes $Ca_p[Cm(OH)_n]^{3+2p-n}$ [11].

SOLUBILITY AND AQUEOUS SPECIATION OF NEODYMIUM AND CURIUM IN DILUTE TO CONCENTRATED NaCl, $MgCl_2$, AND $CaCl_2$ SOLUTIONS

In order to derive a comprehensive thermodynamic model for the system M(III)–H^+–Na^+–Mg^{2+}–Ca^{2+}–Cl^-–OH^-–H_2O at 25 °C, valid over the entire range of ionic strength and pH, the solubility of Nd(III) hydroxide was determined under strict exclusion of CO_2(g) in 0.1, 0.5, 2.5, and 5.0 M NaCl (up to high OH^- concentrations of 0.1–4.0 M) and in 0.25, 1.0, 2.5, and 3.5 M $MgCl_2$ and $CaCl_2$ (up to maximum pH_c, limited to values around 9 and 12, respectively, by the solubility of magnesium and calcium hydroxides or hydroxychlorides). The complementary information on the aqueous speciation, from the TRLFS studies mentioned above, is also taken into account. For calculations with the ion interaction model of Pitzer, the widely accepted data reported by Harvie et al. [2] are used for the matrix components. All calculations and equilibrium constants are given on the molal con-

centration scale. Conversion factors to calculate m_i [mol·(kg H_2O)$^{-1}$] from the molar concentrations c_i [M = mol l^{-1}] are taken from [6].

Experimental

The solid Nd(III) hydroxide used in the present study was prepared under CO_2-free argon atmosphere by hydration of crystalline Nd_2O_3(cr) (Merck) in pure water (actinide and lanthanide oxides M_2O_3(cr) are not stable in aqueous solution and transform into the hydroxides [4,35,36]). The solid was stored for about three months under water. It clearly showed the known XRD pattern of $Nd(OH)_3$(cr) (JCPDS-File 70-0214). The experimental and analytical procedures and the chemicals used to prepare the matrix solutions were the same as in previous studies and described therein [10,11]. The samples for the solubility measurements were prepared and stored at 22 ± 2 °C in an Ar glove box. After equilibration times of 6–150 days and phase separation by either 10 kD ultrafiltration (pore size ca. 1.5 nm) or ultracentrifugation at 90 000 rpm (ca. 5×10^5 g) the samples were analyzed for H^+ and Nd concentrations. The latter were measured by inductively coupled plasma-mass spectroscopy (ICP-MS) (ELAN 6100 Perkin Elmer); detection limit: 10^{-10}–10^{-9} M, depending on the concentration of the background electrolyte. The H^+ concentrations in the NaCl, $MgCl_2$, and $CaCl_2$ solutions (molar scale: $pH_c = -\lg c_{H^+}$; molal scale: $pH_m = -\lg m_{H^+}$) were determined with combination pH electrodes (type ROSS, Orion) calibrated as described in detail in previous papers [1,10,11]. The H^+ concentration in NaCl–NaOH solutions is calculated from the given OH^- concentration (for $[OH^-] > 0.01$ M) and the conditional ion product of water.

XRD and scanning electron microscopy-energy-dispersive spectrometry (SEM-EDS) analysis at the end of the solubility experiments gave no indication for the transformation of the initial $Nd(OH)_3$(s) into a chloride-containing solid phase. The solubility-limiting solid is the same throughout the experiments in the dilute chloride media to 5.0 M NaCl and 3.5 M $MgCl_2$ and $CaCl_2$. This is further confirmed by the constant solubility after short and long equilibration times and by the consistent value of $\lg {}^*K^\circ_{s,0} = 17.2 \pm 0.4$ calculated for $I = 0$ from the H^+ and Nd^{3+} concentrations and the well-known interaction coefficients of these ions [2,14,22]. However, this was not the case in an additional study in 4.5 M $MgCl_2$ where SEM-EDS and the significantly diminished XRD pattern of $Nd(OH)_3$(cr) indicated the transformation into an amorphous $Nd(OH)_{3-x}Cl_x$(s) phase with lower solubility. These results are not further discussed.

Solubility of $Nd(OH)_3$(s): Comparison with literature data

In a review of the earlier literature on the solubility and hydrolysis of the lanthanides, Baes and Mesmer [15] recommended a solubility constant of $\lg {}^*K^\circ_{s,0} = 18.6$ for $Nd(OH)_3$(s) and hydrolysis constants of $\lg {}^*\beta^\circ_{1n}(Nd(OH)_n^{3-n}) = -8.0, -16.9, -26.5$, and -37.1 for n = 1–4 and $\lg {}^*\beta^\circ_{22}(Nd_2(OH)_2^{4+}) = -13.86$ (speciation calculations with this constant from potentiometric titration show that the dimer is not relevant at solubility equilibrium conditions). The value of $\lg {}^*\beta^\circ_{11} = -8.0$ appears too small compared to mean values for Eu(III), $\lg {}^*\beta^\circ_{11}$, -7.5 ± 0.4 [37] and -7.64 ± 0.04 [38], or $\lg {}^*\beta^\circ_{11} = -7.2 \pm 0.5$ for Am(III) and Cm(III) [6]. The data for Eu(III), Am(III), and Cm(III) are based on a much larger number of experimental studies and methods. The hydrolysis constants for n = 2 and 3 were interpolated from $\lg {}^*\beta^\circ_{11} = -8.0$ and $\lg {}^*\beta^\circ_{14} = -37.1$, but the equilibrium constant for the tetrahydroxide complex is overestimated by several orders of magnitude. The value of $\lg K^\circ_{3-4} = 3.4$ derived by Baes and Mesmer [15] from solubility data for $Nd(OH)_3$(s) in NaOH solutions must be due to analytical problems or experimental shortcomings in the underlying solubility studies [39,40] which report concentrations of 10^{-5} to 10^{-4} M in the range of the solubility minimum to high pH. Neither the solubility of $Am(OH)_3$(s) (Fig. 1), with $\lg K^\circ_{3-4} = -0.5$, nor our results for $Nd(OH)_3$(s) (Fig. 2) show an indication for a solubility increase up to pH 14. The solubility curves of $Nd(OH)_3$(s) and $Am(OH)_3$(s) in 0.1 M

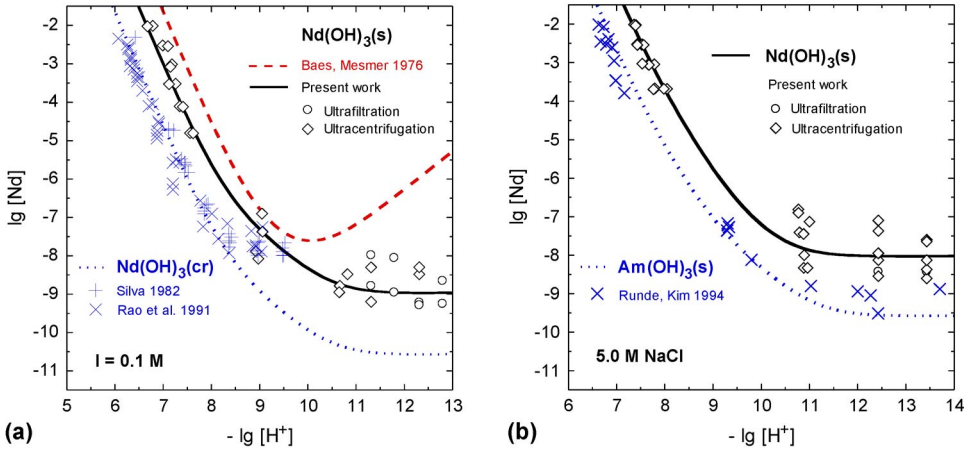

Fig. 2 Solubility of Nd(III) hydroxide at 25 °C. (a) Comparison of data for aged $Nd(OH)_3(s)$ (p.w.) and crystalline $Nd(OH)_3(cr)$ [23,41] at I = 0.1 M; (b) Comparison of data for aged $Nd(OH)_3(s)$ (p.w.) and $Am(OH)_3(s)$ [28] in 5.0 M NaCl. The solid and dotted lines are calculated with $lg^*K°_{s,0}$ = 17.2 and 15.6, respectively, and the hydrolysis constants selected for Nd(III) and Am(III) (SIT model). The dashed line in Fig. 2a is calculated with the solubility and hydrolysis constants recommended by Baes and Mesmer [15].

NaCl or $NaClO_4$ (Figs. 1a and 2a) and in 5.0 M NaCl (Fig. 2b), show the same dependence on pH, just shifted in parallel by about 1.5 lg-units. For these reasons, it is more convenient to use the Am(III)/Cm(III) data as analogs for Nd(III), or the slightly different values of $lg^*\beta°_{11} = -7.4 \pm 0.4$ and $lg^*\beta°_{12} = -15.7 \pm 0.7$ derived from our solubility study with $Nd(OH)_3(s)$.

In later reviews of thermodynamic data for the solid lanthanide hydroxides, Diakonov et al. [35,36] pointed out that the solubility constant $lg^*K°_{s,0}$ = 18.6 recommended by Baes and Mesmer [15] refers to highly soluble amorphous precipitates. From their compilation of published data, they calculated mean values of $lg^*K°_{s,0} = 18.66 \pm 0.55$ for fresh, amorphous precipitates of $Nd(OH)_3(s)$ and 16.02 ± 0.37 for aged and crystalline $Nd(OH)_3(s)$ [35,36]. The solubility constant of the $Nd(OH)_3(s)$ phase used in the present work ($lg^*K°_{s,0} = 17.2 \pm 0.4$) lies between these values. Figure 2a shows our results in 0.1 M NaCl in comparison with the solubility calculated with the equilibrium constants proposed by Baes and Mesmer [15] (dashed line) and the data reported by Silva [23] and Rao et al. [41] for $Nd(OH)_3(cr)$ at 25 °C in 0.1 M $NaClO_4$ and 0.1 M NaCl, respectively. The latter authors prepared well-crystalline Nd(III) hydroxide phases in 5 M NaOH at 90 °C. The solubility determined with this solid at pH 6–8, is in the range of the data for crystalline/aged $Am(OH)_3(s)$ ($lg^*K°_{s,0} = 15.6 \pm 0.6$) and 1–2 lg-units lower than the data obtained for $Nd(OH)_3(s)$ in the present work. This may be explained by a difference in particle/crystallite size. The present results correspond to a less-crystalline solid phase consisting of smaller particles. However, the solubility data determined by Silva [23] and Rao et al. [41] at pH 8.5–9.5 approach our results, indicating that these values refer to smaller particles included in their bulk crystalline solid (comparable to the particle size of the $Nd(OH)_3(s)$ solid used in our study). Similar particle size effects are known for hydrous Th(IV) oxides and discussed in length in [7].

Solubility of $Nd(OH)_3(s)$ and Cm(III)–TRLFS in NaCl and NaCl–NaOH solutions

The experimental solubility data for $Nd(OH)_3(s)$ in 0.1, 0.5, 2.5, and 5.0 M NaCl (Fig. 3) can be described with the simple speciation scheme known for trivalent actinides, i.e., with Nd^{3+} and mononuclear hydrolysis species $Nd(OH)_n^{3-n}$ (n = 1, 2, and 3). The large scatter of the data at $pH_m > 9$ is an indication that the measured concentrations are affected by small (1–2 nm) polymers. On the one hand, uncharged species like $Nd(OH)_3(aq)$ and $Nd_m(OH)_{3m}(aq)$ have a high tendency toward sorption on the

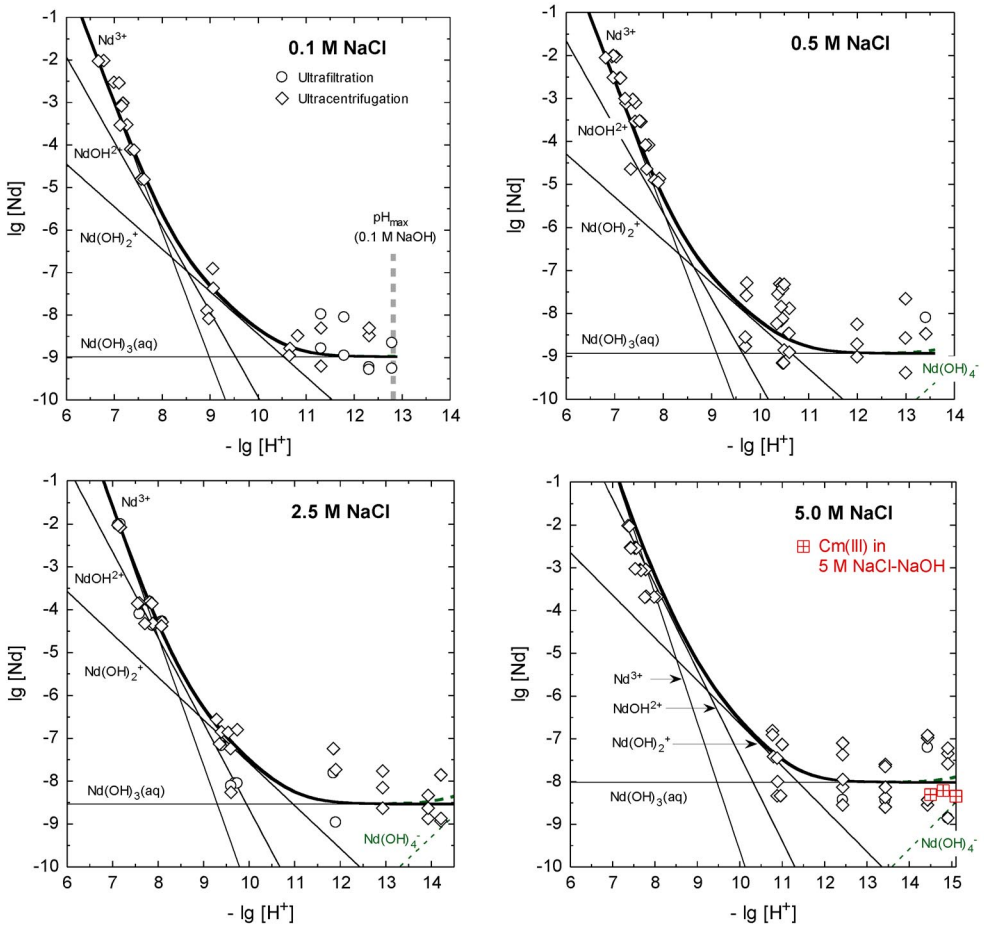

Fig. 3 Solubility of $Nd(OH)_3(s)$ in 0.1, 0.5, 2.5, and 5.0 M NaCl (m_{NaCl} = 0.10, 0.51, 2.64, 5.61 mol kg^{-1}); experimental data (molal scale) and Pitzer model calculation (thick lines: total Nd concentrations, thin lines: contributions of the different species). The aqueous Cm(III) concentrations determined after ultrafiltration in 5.0 M NaCl–NaOH solutions are shown as squares with cross inside.

vessel walls or filter surface, on the other hand, incomplete removal of small polymers by ultrafiltration or ultracentrifugation may lead to increased total Nd concentrations. However, even up to high OH^- concentrations in 5 M NaCl–NaOH, there is no indication for a solubility increase due to the formation of anionic hydroxide complexes. This is consistent with the equilibrium constant derived above for $Am(OH)_4^-$ from the solubility of $Am(OH)_3(s)$ in 0–10 M KOH [29] (c.f., dashed concentration lines calculated for $Nd(OH)_4^-$). It is also consistent with the observation that TRLFS shows no discernible Cm(III) emission spectrum at $[OH^-]$ = 1–4 M in 5 M NaCl–NaOH [11]. The curium concentrations measured after 10 kD ultrafiltration, lg [Cm] = –8.3 ± 0.1 (c.f., squares in Fig. 3), should be sufficient for a clear TRLFS emission spectrum, but obviously the dissolved curium is almost completely present as $Cm_m(OH)_{3m}$ polymers which show no fluorescence emission bands [33,34].

Solubility of $Nd(OH)_3(s)$ and Cm(III)–TRLFS in $MgCl_2$ and alkaline $CaCl_2$ solutions

The results of the solubility experiments in 0.25, 1.0, 2.5, and 3.5 M $MgCl_2$ (pH_m < 9) and $CaCl_2$ (pH_m < 12) are shown in Fig. 4. In the overlapping pH_m regions the solubilities in equimolar $MgCl_2$

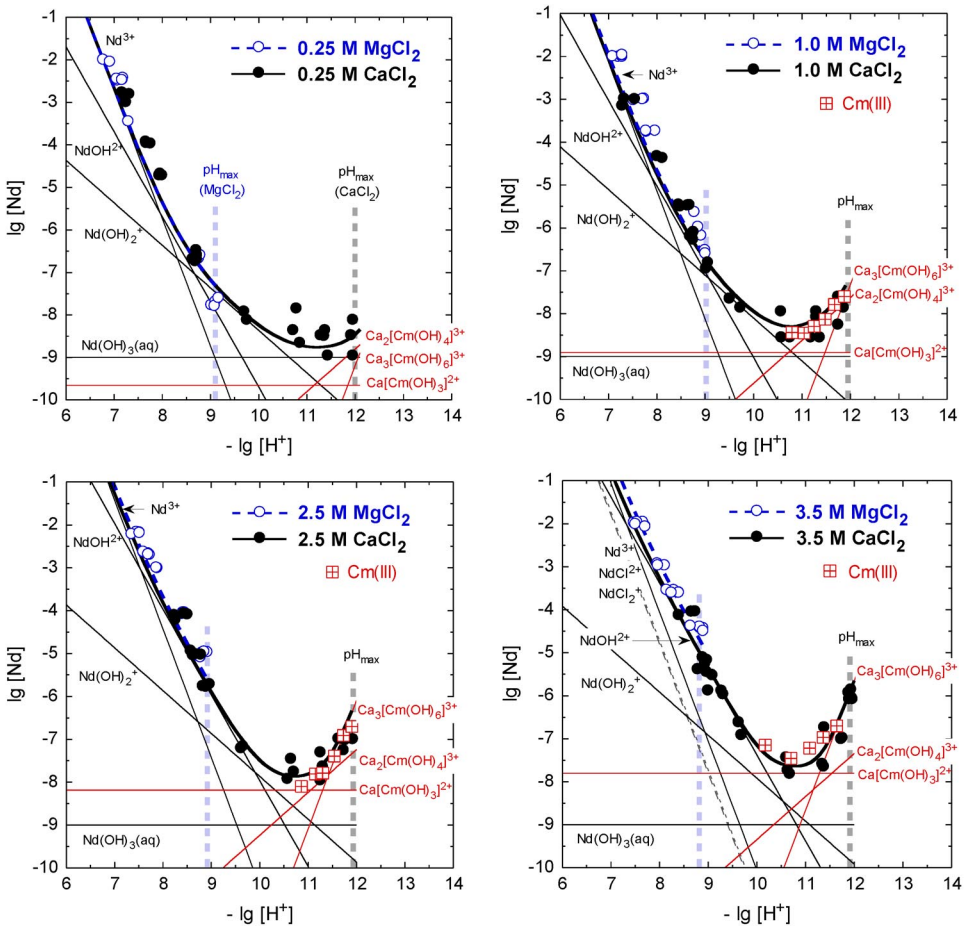

Fig. 4 Solubility of $Nd(OH)_3$(s) in 0.25, 1.0, 2.5, and 3.5 M $MgCl_2$ and $CaCl_2$ (m_{MgCl2} = 0.25, 1.02, 2.67, and 3.86 mol kg^{-1}, m_{CaCl_2} = 0.25, 1.02, 2.68, and 3.91 mol kg^{-1}); experimental data (molal scale) and Pitzer model calculation (fat lines: total Nd concentrations, thin lines: contributions of the different species). The Cm(III) concentrations determined after ultrafiltration in the TRLFS samples are shown as squares with cross inside.

and $CaCl_2$ solutions are identical or close to each other. (Note that Fig. 4 shows molal values of lg {[Nd]/mol kg^{-1}} plotted vs. $pH_m = -$ lg {[H^+]/mol kg^{-1}}, and that the conversion factors from molarity to molality and also lg γ_{H^+} in eqs. 1 and 2 diverge to a certain extent with increasing electrolyte concentration, either 0.25, 1.02, 2.67, 3.86 m $MgCl_2$ or 0.25, 1.02, 2.68, 3.91 m $CaCl_2$). Contrary to the solubility at high pH in NaCl solutions, the solubility of $Nd(OH)_3$(s) in 1.0, 2.5, and 3.5 M $CaCl_2$ clearly increases in the range pH_m = 11–12. The higher the $CaCl_2$ concentrations the more pronounced is this effect. Another noteworthy difference compared to the results in alkaline NaCl media is the fact that the data in alkaline $CaCl_2$ solutions are much less scattered, indicating that the measured Nd concentrations are caused by well-defined ionic species.

These observations and conclusions are confirmed by TRLFS emission spectra with $[Cm]_{tot} = 2 \times 10^{-7}$ M in 0.1–3.5 M $CaCl_2$ at $pH_m \approx 11.7$ and in three sets at constant ionic strength (1.0, 2.5, and 3.5 M $CaCl_2$) and varying pH_m [11] (Fig. 5). Peak deconvolution and the evaluation of the pH dependence of the spectroscopic data showed that Cm(III) complexes with three, four, and six OH^- ligands are formed (λ_{max} = 607.5, 609.9, and 614.7 nm, respectively). As these species are absent in NaCl–NaOH media, although the Cm(III) concentrations after 10 kD ultrafiltration are similar to those

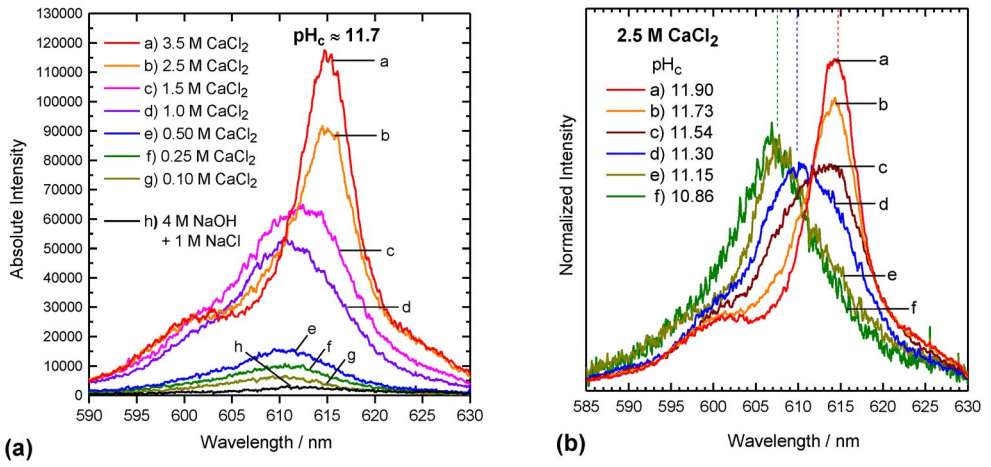

Fig. 5 TRLFS emission spectra of 2×10^{-7} M Cm(III) in alkaline $CaCl_2$ solutions, (a) at $pH_c \approx 11.7$ in 0.1–3.5 M $CaCl_2$ (original spectra), (b) in 2.5 M $CaCl_2$ with pH_c varied in the range 10.8–11.9 (spectra normalized with regard to the total fluorescence counts under the peak area). Further spectra in 1.0 and 3.5 M $CaCl_2$ and a detailed discussion are given in [11].

in 1.0 M $CaCl_2$ (about 10^{-8} M), they must be stabilized by the association of Ca^{2+} ions. This also explains the strong increase of the intensity of the emission bands in 0.1–1.0 M $CaCl_2$ (Fig. 5a) which are caused by the tri- and tetrahydroxide complexes $Ca_x[Cm(OH)_3]^{2x}$ and $Ca_y[Cm(OH)_4]^{2y-1}$. The hexahydroxide complex $Ca_z[Cm(OH)_6]^{2z-3}$ dominates at higher $CaCl_2$ concentrations and $pH_m > 11.5$. The spectroscopic speciation is supported by the Cm(III) concentrations determined after 10 kD ultrafiltration of the TRLFS samples in 1.0, 2.5, and 3.5 M $CaCl_2$ (c.f., squares in Fig. 4). These concentrations, $[Cm(III)]_{aq}$ in equilibrium with colloidal $Cm(OH)_3$(am), clearly increase from pH_m 10.5 to 12 and also with increasing $CaCl_2$ concentration. At $pH_m > 11.5$ in 3.5 M $CaCl_2$, the curium ($[Cm]_{tot} = 2 \times 10^{-7}$ M) is completely dissolved as ionic species. It may be accidental that these Cm(III) concentrations coincide with the solubility data for $Nd(OH)_3$(s), i.e., that the solubility constant of small colloidal $Cm(OH)_3$(am) particles is equal to that of our $Nd(OH)_3$(s) phase. However, the finding that the dependence on the $CaCl_2$ concentration and pH is the same for Cm(III) and Nd(III) is not unexpected as it confirms the usual (qualitative and quantitative) analogy for the aqueous complexes of Cm^{3+} and Nd^{3+}.

The extremely different chemical and spectroscopic behavior of Cm(III) in alkaline $CaCl_2$ solutions compared to that in pure NaOH and NaCl–NaOH solutions and the analogous discrepancies for the solubility of $Nd(OH)_3$(s) in these media cannot be explained by binary hydroxide complexes $M(OH)_n^{3-n}$ and different ion interaction coefficients with Ca^{2+} compared to those with Na^+. A thermodynamic model valid for both Ca-free and -containing solutions requires the formulation as ternary complexes $Ca_p[M(OH)_n]^{2p+3-n}$. The number of associated Ca^{2+} ions cannot be determined independently with the presently available methods. However, in analogy to the M(IV) complexes $Ca_3[Zr(OH)_6]^{4+}$ and $Ca_4[Th(OH)_8]^{4+}$, where the number of Ca^{2+} ions in the second shell and the coordination structure could be determined by EXAFS [9] (one Ca^{2+} ion bound to two OH^- ligands via edges of the $[M(OH)_n^{z-}]$ coordination polyhedra), it appears reasonable to assume the stoichiometries $Ca[Cm(OH)_3]^{2+}$, $Ca_2[Cm(OH)_4]^{3+}$, and $Ca_3[Cm(OH)_6]^{3+}$. In our recent study [11], the SIT was used to calculate the formation constants $\lg^*\beta^\circ_{p,1,n}$ and ion interaction coefficients for these ternary complexes from the spectroscopic data for Cm(III) in 1.0, 2.5, and 3.5 M $CaCl_2$ and the solubility constant for colloidal $Cm(OH)_3$(am) which is equal to that of $Nd(OH)_3$(s):

$$p\mathrm{Ca}^{2+} + \mathrm{Cm}^{3+} + n\mathrm{H_2O} \Leftrightarrow \mathrm{Ca}_p[\mathrm{Cm(OH)}_n]^{2p+3-n} + n\mathrm{H}^+$$

$$\mathrm{lg}^*\beta^\circ_{1,1,3} = -26.3 \pm 0.5,\ \ \varepsilon(\mathrm{Ca[Cm(OH)_3]}^{2+}, \mathrm{Cl}^-) = 0.05 \pm 0.04 \text{ kg mol}^{-1}$$

$$\mathrm{lg}^*\beta^\circ_{2,1,4} = -37.2 \pm 0.6,\ \ \varepsilon(\mathrm{Ca_2[Cm(OH)_4]}^{3+}, \mathrm{Cl}^-) = 0.29 \pm 0.07 \text{ kg mol}^{-1}$$

$$\mathrm{lg}^*\beta^\circ_{3,1,6} = -60.7 \pm 0.5,\ \ \varepsilon(\mathrm{Ca_3[Cm(OH)_6]}^{3+}, \mathrm{Cl}^-) = 0.00 \pm 0.06 \text{ kg mol}^{-1}$$

The SIT coefficients for the other ions involved are given in the NEA-TDB [3–6]: $\varepsilon(\mathrm{M}^{3+}, \mathrm{Cl}^-) = 0.23 \pm 0.02$ for M = Nd, Cm, and Am, $\varepsilon(\mathrm{Ca}^{2+}, \mathrm{Cl}^-) = 0.14 \pm 0.01$ and $\varepsilon(\mathrm{H}^+, \mathrm{Cl}^-) = 0.12 \pm 0.01$ kg mol^{-1}. In the present study, the TRLFS results are re-evaluated with the Pitzer equations. As $\mathrm{lg}^*\beta'_{p,1,n}$ values at only three different ionic strengths do not allow a reasonable fit of all parameters, the constants at $I = 0$ derived with the SIT are used as fixed values. Following a recommendation to keep consistency between SIT and Pitzer model [20], the Pitzer parameters $\beta^{(1)}(\mathrm{Ca}_p[\mathrm{Cm(OH)}_n]^{2p+3-n}, \mathrm{Cl}^-)$ for the charge types 2:1 and 3:1 are fixed at 1.6 and 4.3 kg mol^{-1}, respectively. Including the data for these ternary complexes in a comprehensive thermodynamic model (c.f., discussion below in the final section) allows the geochemical modeling of the solubility and hydrolysis of trivalent actinides and Nd(III) over the entire pH range in dilute to concentrated NaCl, $\mathrm{MgCl_2}$, and $\mathrm{CaCl_2}$ media at 25 °C. This is illustrated in Figs. 3 and 4, where the total solubility of $\mathrm{Nd(OH)_3(s)}$ and the different species contributions calculated with the Pitzer approach are shown as fat and thin lines, respectively. Corresponding calculations with the SIT are practically identical for $I \leq 3$ mol kg^{-1}, even at high ionic strength they deviate less than 0.5 lg-units from the Pitzer model calculations.

Thermodynamic model for solid hydroxides and aqueous complexes of trivalent actinides and Nd(III) in the system M(III)–H^+–Na^+–Mg^{2+}–Ca^{2+}–Cl^-–OH^-–H_2O (25 °C)

The standard-state equilibrium constants (I = 0, 25 °C) for solid hydroxides and aqueous Am(III)/Cm(III) and Nd(III) complexes in NaCl, $\mathrm{MgCl_2}$, and $\mathrm{CaCl_2}$ solutions are summarized in Table 1; ion interaction coefficients for the aqueous species are listed in Tables 2 and 3. The Pitzer parameters (Table 2) refer to auxiliary data reported by Harvie et al. [2] for the seawater salt system, SIT coefficients for the ions of the matrix components are taken from the NEA-TDB [3–6]. The ion interaction parameters for Nd^{3+} ions (equal to those for An^{3+} ions [6,21,22]) are well known from data in binary $\mathrm{NdCl_3}$ and ternary $\mathrm{NdCl_3}$–NaCl and $\mathrm{NdCl_3}$–$\mathrm{CaCl_2}$ systems [14,22]. The equilibrium constants and Pitzer parameters for chloride complexes are based on TRLFS data for Cm(III) [22,30].

The thermodynamic data selected in the NEA-TDB [6] for solid Am(III) hydroxides and the hydrolysis constants $\mathrm{lg}^*\beta^\circ_{1n}$ (n = 1–3) for Am(III)/Cm/III) are well ascertained. The solubility constant of the aged $\mathrm{Nd(OH)_3(s)}$ phase used in the present study, $\mathrm{lg}^*K^\circ_{s,0} = 17.2 \pm 0.4$, and the value of 16.0 ± 0.4 proposed by Diakonov et al. [35,36] for aged and crystalline $\mathrm{Nd(OH)_3(s)}$ are close to the values selected in the NEA-TDB [6] for amorphous and aged/crystalline $\mathrm{Am(OH)_3(s)}$. The very high values of $\mathrm{lg}^*K^\circ_{s,0}[\mathrm{Nd(OH)_3(am)}] = 18.66 \pm 0.55$ [35,36] or 18.6 [15] are probably not appropriate for long-term model calculations. The hydrolysis constants $\mathrm{lg}^*\beta^\circ_{11} = -7.4 \pm 0.4$ and $\mathrm{lg}^*\beta^\circ_{12} = -15.7 \pm 0.7$ derived from our solubility study with $\mathrm{Nd(OH)_3(s)}$ are in the range of the values selected in the NEA-TDB [6] from numerous studies and different experimental methods for Am(III) and Cm(III). The previously reported SIT coefficients [6] and particularly the Pitzer parameters [18,22] for $\mathrm{M(OH)^{2+}/Cl^-}$ and $\mathrm{M(OH)_2^+/Cl^-}$ are mainly based on a TRLFS study in 0–6 m NaCl [31]. Their application to $\mathrm{MgCl_2}$ and $\mathrm{CaCl_2}$ solutions of higher ionic strength considerably overpredicts the formation of the dihydroxide complex $\mathrm{M(OH)_2^+}$ and hence the solubility in the range $\mathrm{pH_m}$ = 8–11. The Pitzer parameters for these species have therefore been adjusted to the present solubility data for $\mathrm{Nd(OH)_3(s)}$ and literature data for the solubility of aged $\mathrm{Am(OH)_3(s)}$ in 0.1, 0.6, and 5.0 M NaCl [26,28]. Ternary parameters for cationic M(III) species in $\mathrm{MgCl_2}$ solutions are set equal to the corresponding parameters with Ca^{2+}. The SIT coefficient for the monohydroxide complex,

$\varepsilon[M(OH)^{2+}, Cl^-]$ = –0.04 ± 0.07 kg mol^{-1} [6] can be retained, but the value of $\varepsilon[M(OH)_2{}^+, Cl^-]$ has to be revised, from –0.27 ± 0.20 [6] into –0.06 ± 0.08 kg mol^{-1}.

Table 1 Equilibrium constants (I = 0, 25 °C) for the solid hydroxides and aqueous complexes of Am(III)/Cm(III) and Nd(III).

Solubility: $\lg {}^*K^\circ_{s,0}$ $[M(OH)_3(s) + 3H^+ \Leftrightarrow M^{3+} + 3H_2O]$				
$Am(OH)_3$(cr/aged)	15.6 ± 0.6	[6]	$Nd(OH)_3$(cr/aged)	16.0 ± 0.4 [35]
$Am(OH)_3$(am):	16.9 ± 0.8	[6]	$Nd(OH)_3$(s)	17.2 ± 0.4 p.w.
Chloride complexes: $\lg \beta^\circ_n$ $[M^{3+} + nCl^- \Leftrightarrow MCl_n{}^{3-n}]$				
$AnCl^{2+}$ (Am/Cm)	0.24 ± 0.03	[6,22]	$NdCl^{2+}$: analogous Cm value	
$AnCl_2{}^+$ (Am/Cm)	–0.74 ± 0.05	[6,22]	$NdCl_2{}^+$: analogous Cm value	
Hydroxide complexes: $\lg {}^*\beta^\circ_{1n}$ $[M^{3+} + nH_2O \Leftrightarrow M(OH)_n{}^{3-n} + nH^+]$				
$An(OH)^{2+}$ (Am/Cm)	–7.2 ± 0.5	[6]	$Nd(OH)^{2+}$:	–7.4 ± 0.4 p.w.
$An(OH)_2{}^+$ (Am/Cm)	–15.1 ± 0.7	[6]	$Nd(OH)_2{}^+$:	–15.7 ± 0.7 p.w.
$Am(OH)_3$(aq)	–26.2 ± 0.5	[6]	$Nd(OH)_3$(aq):	analogous Am value
$Am(OH)_4{}^-$	–40.7 ± 0.7	p.w.	$Nd(OH)_4{}^-$:	analogous Am value
Ca–M(III)–OH complexes: $\lg {}^*\beta^\circ_{p,1,n}$ $\{pCa^{2+} + M^{3+} + nH_2O \Leftrightarrow Ca_p[M(OH)_n]^{2p+3-n} + nH^+\}$				
$Ca[Cm(OH)_3]^{2+}$	–26.3 ± 0.5	[11], p.w.	$Ca[Nd(OH)_3]^{2+}$: analogous Cm value	
$Ca_2[Cm(OH)_4]^{3+}$	–37.2 ± 0.6	[11], p.w.	$Ca_2[Nd(OH)_4]^{3+}$: analogous Cm value	
$Ca_3[Cm(OH)_6]^{3+}$	–60.7 ± 0.5	[11], p.w.	$Ca_3[Nd(OH)_6]^{3+}$: analogous Cm value	

Table 2 Ion interaction (Pitzer) coefficients for M(III) species (M = Am, Cm, Pu, and Nd) in chloride media at 25 °C; $\beta^{(0)}{}_{ik}$, $\beta^{(1)}{}_{ik}$, λ_{ik}, and θ_{ij} in [kg mol^{-1}], $C^\phi{}_{ik}$ and ψ_{ijk} in [kg^2 mol^{-2}].

Binary Pitzer parameters					Ternary Pitzer parameters			
i	k	$\beta^{(0)}{}_{ik}$	$\beta^{(1)}{}_{ik}$	$C^\phi{}_{ik}$	j	θ_{ij}	ψ_{ijk}	Ref.
M^{3+}	Cl^-	0.5856	5.60	–0.016	Na^+	0.10	0	[22]
					Ca^{2+}/Mg^{2+}	0.20	0	[22]
MCl^{2+}	Cl^-	0.593	3.15	–0.006	Na^+	0	0	[22]
					Ca^{2+}/Mg^{2+}	–0.014	0	[22]
$MCl_2{}^+$	Cl^-	0.516	1.75	0.010	Na^+	0	0	[22]
					Ca^{2+}/Mg^{2+}	–0.196	0	[22]
$M(OH)^{2+}$	Cl^-	0.055	1.81	0	Na^+	0	0	[18]
					Ca^{2+}/Mg^{2+}	0	0.04	p.w.
$M(OH)_2{}^+$	Cl^-	–0.13	0	0	Na^+	0	0	p.w.
					Ca^{2+}/Mg^{2+}	0.29	0.07	p.w.
$M(OH)_4{}^-$	K^+/Na^+	0	0	0	Cl^-/OH^-	0	0	p.w.
	Ca^{2+}/Mg^{2+}	0	0	0	Cl^-	0	0	p.w.[b]
$Ca[M(OH)_3]^{2+}$	Cl^-	0.21	1.6[a]	0	Ca^{2+}	0	0	p.w.
$Ca_2[M(OH)_4]^{3+}$	Cl^-	0.70	4.3[a]	0	Ca^{2+}	0	0	p.w.
$Ca_3[M(OH)_6]^{3+}$	Cl^-	0.37	4.3[a]	0	Ca^{2+}	0	0	p.w.
$M(OH)_3$(aq)	Na^+	λ_{ik} = –0.2						[22]
		λ_{ik} = 0 for k = K^+, Ca^{2+}, Mg^{2+}, Cl^-, OH^-						p.w.[b]

[a]Fixed value for the corresponding charge type, according to [20].
[b]Strong interaction with Ca^{2+} must be expressed in terms of Ca–M(III)–OH complex formation, interaction with Mg^{2+} is not relevant (pH_m < 9 in $MgCl_2$ solutions).

Table 3 Ion interaction (SIT) coefficients ε_{ik} [kg mol^{-1}] for M(III) species (M = Am, Cm, Pu, and Nd) in chloride media at 25 °C.

i	k	ε_{ik} [kg mol^{-1}]		i	k	ε_{ik} [kg mol^{-1}]	
M^{3+}	Cl^-	0.23 ± 0.02	[6]	$M(OH)_3(aq)$	Cl^-/OH^-	0	p.w.
$M(OH)^{2+}$	Cl^-	–0.04 ± 0.07	[6]	$M(OH)_3(aq)$	Na^+	–0.17 ± 0.10	p.w.
$M(OH)_2^+$	Cl^-	–0.06 ± 0.08	p.w.	$M(OH)_3(aq)$	K^+	0	p.w.
$Ca[M(OH)_3]^{2+}$	Cl^-	0.05 ± 0.04	[11]	$M(OH)_3(aq)$	Ca^{2+}/Mg^{2+}	0[a]	p.w.
$Ca_2[M(OH)_4]^{3+}$	Cl^-	0.29 ± 0.07	[11]	$M(OH)_4^-$	K^+/Na^+	–0.03 ± 0.05	p.w.
$Ca_3[M(OH)_6]^{3+}$	Cl^-	0.00 ± 0.06	[11]	$M(OH)_4^-$	Ca^{2+}/Mg^{2+}	0[a]	p.w.

[a]Strong interaction with Ca^{2+} must be expressed in terms of Ca–M(III)–OH complex formation, interaction with Mg^{2+} is not relevant because $pH_m < 9$ in $MgCl_2$ solutions.

The NEA-TDB value of $\lg^*\beta^\circ_{13}[Am(OH)_3(aq)] = -26.2 \pm 0.5$ [6], exclusively based on solubility data for $Am(OH)_3(s)$ in alkaline solutions of low ionic strength, is adopted in the present work for $Nd(OH)_3(aq)$. The somewhat increased solubility of $Am(OH)_3(s)$ and $Nd(OH)_3(s)$ at pH 10–14 in 5.0 M NaCl compared to lower ionic strength (c.f., Figs. 2 and 3) may be described (for practical purposes) by introducing an interaction coefficient for the neutral $M(OH)_3(aq)$ complex, e.g., a Pitzer coefficient of $\lambda(M(OH)_3(aq), Na^+) = -0.2$ kg mol^{-1} [22] (Table 2), corresponding to a SIT coefficient of $\varepsilon(M(OH)_3(aq), Na^+) = -0.17$ kg mol^{-1} (Table 3). However, the large scatter of the measured Am or Nd concentrations and the absence of a Cm(III) emission band in alkaline NaCl solutions indicate that these concentrations are rather caused by small polymers than by the mononuclear complex $M(OH)_3(aq)$.

The formation constant for the tetrahydroxide complex is derived in the present work from the solubility increase of aged $Am(OH)_3(s)$ in 0–10 M KOH [29] (Fig. 1b). This effect is well described with $\lg^*\beta^\circ_{14} = -40.7 \pm 0.7$ and $\varepsilon(Am(OH)_4^-, K^+) = -0.03 \pm 0.05$ kg mol^{-1} or equivalently with the Pitzer model and all parameters for the interactions of $Am(OH)_3(aq)$ and $Am(OH)_4^-$ with K^+ and/or OH^- equal to zero. However, the KOH matrix solutions used in [29] were saturated with $Ca(OH)_2(s)$ and contained small but definite Ca^{2+} concentrations—vice versa than in alkaline $CaCl_2$ solutions with rather high Ca^{2+} but low OH^- concentrations ($pH_m < 12$) where the solubility increase of $Nd(OH)_3(s)$ is consistently described with the data derived for $Ca[Cm(OH)_3]^{2+}$, $Ca_2[Cm(OH)_4]^{3+}$, and $Ca_3[Cm(OH)_6]^{3+}$ from the TRLFS study with Cm(III). It cannot be excluded that the solubility increase of $Am(OH)_3(s)$ in 3–10 M KOH might also be caused by ternary Ca–Am(III)–OH complexes, but a fit including species like $Ca[Am(OH)_3]^{2+}$ or $Ca[Am(OH)_4]^+$ and Pitzer parameters for their interactions with OH^- and K^+ would be highly speculative.

Equilibrium constants for Pu(III) are much less ascertained than for Am(III) or Cm(III). The solubility constant determined by Felmy et al. [21] for fresh precipitates of $Pu(OH)_3(s)$, $\lg^*K^\circ_{s,0} = 15.8 \pm 0.8$, the only experimental value available for Pu(III) hydroxide, is accepted in the NEA-TDB [5,6]. As only the first hydrolysis constant is known ($\lg^*\beta^\circ_{11}(Pu(OH)^{2+}) = -6.9 \pm 0.3$ [5,6]), unknown data for other Pu(III) complexes must be adopted from the Am(III)/Cm(III) analogs. This approach was successfully applied to plutonium solubilities under reducing conditions in $MgCl_2$ and $CaCl_2$ solutions in contact with iron powder [12].

REFERENCES

1. M. Altmaier, V. Metz, V. Neck, R. Müller, Th. Fanghänel. *Geochim. Cosmochim. Acta* **67**, 3595 (2003).
2. C. F. Harvie, N. Møller, J. H. Weare. *Geochim. Cosmochim. Acta* **48**, 723 (1984).
3. I. Grenthe, J. Fuger, R. J. M. Konings, R. J. Lemire, A. B. Muller, C. Nguyen-Trung, H. Wanner (OECD, NEA). *Chemical Thermodynamics Vol. 1, Chemical Thermodynamics of Uranium*, Elsevier, North-Holland, Amsterdam (1992).

4. R. J. Silva, G. Bidoglio, M. H. Rand, P. B. Robouch, H. Wanner, I. Puigdomenech (OECD, NEA). *Chemical Thermodynamics, Vol. 2, Chemical Thermodynamics of Americium*, Elsevier, North-Holland, Amsterdam (1995).
5. R. J. Lemire, J. Fuger, H. Nitsche, P. Potter, M. H. Rand, J. Rydberg, K. Spahiu, J. C. Sullivan, W. J. Ullman, P. Vitorge, H. Wanner (OECD, NEA). *Chemical Thermodynamics, Vol. 4, Chemical Thermodynamics of Neptunium and Plutonium*, Elsevier, North-Holland, Amsterdam (2001).
6. R. Guillaumont, Th. Fanghänel, J. Fuger, I. Grenthe, V. Neck, D. A. Palmer, M. H. Rand (OECD, NEA). *Chemical Thermodynamics, Vol. 5, Update on the Chemical Thermodynamics of Uranium, Neptunium, Plutonium, Americium and Technetium*, Elsevier, Amsterdam (2003).
7. M. H. Rand, J. Fuger, I. Grenthe, V. Neck, D. Rai. *Chemical Thermodynamics, Vol. 11, Chemical Thermodynamics of Thorium*, OECD Nuclear Energy Agency, Paris (2008).
8. V. Neck, M. Altmaier, Th. Fanghänel. *Comptes Rendus Chimie (France)* **10**, 959 (2007).
9. B. Brendebach, M. Altmaier, J. Rothe, V. Neck, M. A. Denecke. *Inorg. Chem*. **46**, 6804 (2007).
10. M. Altmaier, V. Neck, Th. Fanghänel. *Radiochim. Acta* **96**, 541 (2008).
11. Th. Rabung, M. Altmaier, V. Neck, Th. Fanghänel. *Radiochim. Acta* **96**, 551 (2008).
12. M. Altmaier, V. Neck, J. Lützenkirchen, Th. Fanghänel. *Proc. of the Conf. Plutonium Futures: The Science 2008, Dijon, France (2008). Radiochim. Acta* **97**, 187 (2009).
13. L. Ciavatta. *Ann. Chim. (Rome)* **70**, 551 (1980).
14. K. S. Pitzer. *Activity Coefficients in Electrolyte Solutions*, CRC Press, Boca Raton (1991).
15. C. F. Baes Jr., R. E. Mesmer. *The Hydrolysis of Cations*, John Wiley, New York (1976).
16. G. R. Choppin, E. N. Rizkalla. In *Handbook on the Physics and Chemistry of Rare Earths*, K. A. Gschneidner Jr., L. Eyring (Eds.), 18, pp. 559–590, North Holland, Amsterdam (1994).
17. D. Shannon. *Acta Crystallogr., Sect. A* **32**, 751 (1976).
18. V. Neck, Th. Fanghänel, J. I. Kim. Report FZKA 6110, Karlsruhe (1998).
19. Th. Fanghänel, J. I. Kim. *J. Alloys Compd*. **271–273**, 728 (1998).
20. I. Grenthe, I. Puigdomenech. *Modelling in Aquatic Chemistry*, OECD, Nuclear Energy Agency, Paris (1997).
21. A. R. Felmy, D. Rai, J. A. Schramke, J. L. Ryan. *Radiochim. Acta* **48**, 29 (1989).
22. Th. Könnecke, Th. Fanghänel, J. I. Kim. *Radiochim. Acta* **76**, 131 (1997).
23. R. J. Silva. Report LBL-15055, Lawrence Berkeley Laboratory, Berkeley (1982).
24. N. M. Edelstein, J. Bucher, R. J. Silva, H. Nitsche. Report ONWI-399, LBL-15055, Lawrence Berkeley Laboratory, Berkeley (1983).
25. H. Nitsche, N. M. Edelstein. *Radiochim. Acta* **39**, 23 (1985).
26. S. Stadler, J. I. Kim. *Radiochim. Acta* **44–45**, 39 (1988).
27. D. Rai, R. G. Strickert, D. A. Moore, J. L. Ryan. *Radiochim. Acta* **33**, 201 (1983).
28. W. Runde, J. I. Kim. Report RCM 01094, Technische Universität München (1994).
29. P. Vitorge, P. Tran-The. Report EUR 13664, Commission of the European Communities, Luxembourg (1991).
30. Th. Fanghänel, J. I. Kim, R. Klenze, Y. Kato. *J. Alloys Compd*. **225**, 308 (1995).
31. Th. Fanghänel, J. I. Kim, P. Paviet, R. Klenze, W. Hauser. *Radiochim. Acta* **66–67**, 81 (1994).
32. H. Wimmer, R. Klenze, J. I. Kim. *Radiochim. Acta* **56**, 79 (1992).
33. Z. Wang, A. R. Felmy, Y. X. Xia, M. J. Mason. *Radiochim. Acta* **91**, 329 (2003).
34. J. Tits, T. Stumpf, Th. Rabung, E. Wieland, Th. Fanghänel. *Environ. Sci. Technol*. **37**, 3568 (2003).
35. I. I. Diakonov, B. R. Tagirov, K. V. Ragnarsdottir. *Radiochim. Acta* **81**, 107 (1998).
36. I. I. Diakonov, K. V. Ragnarsdottir, B. R. Tagirov. *Chem. Geol.* **151**, 327 (1998).
37. J.-I. Yun, T. Bundschuh, V. Neck, J.-I. Kim. *Appl. Spectrosc.* **55**, 273 (2001).
38. W. Hummel, U. Berner, E. Curti, F. J. Pearson, T. Thoenen. *Nagra/PSI Chemical Thermodynamic Data Base 01/01*, Universal Publishers, Parkland, FL, USA (2002).
39. R. S. Tobias, A. B. Garrett. *J. Am. Chem. Soc*. **80**, 3532 (1958).

40. B. N. Ivanov-Emin, E. N. Sifarova, M. M. Fisher, V. M. Kampos. *Russ. J. Inorg. Chem.* **11**, 258 (1966).
41. L. Rao, D. Rai, A. R. Felmy. *Radiochim. Acta* **72**, 151 (1996).